Renewable and Sustainable Energy Reviews 24 (2013) 73–83

Contents lists available at SciVerse ScienceDirect

Renewable and Sustainable Energy Reviews

journal homepage: www.elsevier.com/locate/rser

Review on the numerical investigations into the design and development of Savonius wind rotors

Sukanta Roy, Ujjwal K. Saha *

Department of Mechanical Engineering, Indian Institute of Technology Guwahati, Guwahati-781 039, India

ARTICLE INFO

Article history:
Received 2 September 2011
Received in revised form
18 March 2013
Accepted 21 March 2013
Available online 10 April 2013

Keywords:
Wind energy
Savonius rotor
Computational fluid dynamics
Turbulence modeling
Soft-computing technique

ABSTRACT

In recent era, research and development activities in the field of renewable energy, especially wind and solar, have been considerably increased, due to the worldwide energy crisis and high global emission. However, the available technical designs are not yet adequate to develop a reliable distributed wind energy converter for low wind speed conditions. The Savonius rotor appears to be particularly promising for such conditions, but suffers from a low efficiency. Till now, a number of experimentations have been carried out in the area of Savonius rotor to increase its efficiency. These large-scale experimentations involve massive costs and hazards. In this context, computational studies have shown a significant importance to carry out the research with large number of physical designs and parameters. Over the past four decades, investigations have been carried out with various computational methodologies and turbulence models to optimize the different parameters and hence the efficiency of these rotors. In the present paper, a detailed review of various computational methods addressing the influence of various operating parameters and augmentation techniques has been reported. From this review study, it is observed that with the selection of a proper computational methodology, the design, performance, and efficiency of a Savonius rotor can be enhanced significantly.

Contents

Abbreviations: ANFIS, adaptive neuro-fuzzy inference system; ANN, artificial neural network; CCS, carbon capture and storage; CFD, computational fluid dynamics; CO_2, carbon di-oxide; DDM, domain decomposition method; DES, detached eddy simulation; DVM, discrete vortex method; FDM, finite difference method; FEM, finite element method; FIS, fuzzy inference system; FVM, finite volume method; HAWT, horizontal axis wind turbine; LES, large eddy simulation; MAC, marker-and-cell; OPAL, optimization library; PIV, particle image velocimetry; RANS, Reynolds averaged Navier Stokes; RBF, radial basis function; RNG, renormalized; SST, shear stress transport; *TSR*, tip speed ratio; VAWT, vertical axis wind turbine.

* Corresponding author. Tel.: +91 361 2582663; fax: +91 361 2690762, 2582699.
E-mail addresses: saha@iitg.ernet.in, saha.cascade@gmail.com (U.K. Saha).

1364-0321/$ - see front matter
http://dx.doi.org/10.1016/j.rser.2013.03.060

1. Introduction

From the beginning of the universe, human society has been based on solar power, both in direct form as solar radiation and in indirect forms as bioenergy, hydro or wind energy. However, with the advancement of civilization, the highly energy contained coal and other fossil fuels have become more prominent up to 1970 due to easy transportation and processing [1]. Beyond 1970, renewable energy sources such as solar, hydro, wind and bioenergy are starting to take control over the energy sectors because of lagging in the sources of conventional fuels. The motivation towards the development of wind energy in 1973 was the high price of oil and concern over the limited fossil-fuel resources. Now, owing to the present scenario of high electricity demand and at the same time need of reduction in the global warming and carbon pollution, the exertion of clean energy and the unlimited potential of wind energy forcing the research and improvement necessities of wind turbines as a source of electricity [2,3].

1.1. Present energy scenario

Coal has been the fastest-growing global source of energy, meeting 47% of new electricity demand. People are interested for introducing carbon capture and storage (CCS) technology to meet the climate change goals by 2020, which hardly seems feasible. That is why, in recent years more emphasis has been given on the clean energy. Biofuels have shown a steady growth; however, only represent 3% of global road transport fuel consumption. Solar and wind power are the fast growing sectors in the renewable energy field. Wind power has experienced dramatic growth over the last decade. The global installed capacity of wind energy at the end of 2010 was around 194 GW, a 17 GW increase from the year 2000. Achieving the goal to cut off global energy-related CO_2 emissions by 2050, requires a doubling (from today's levels) of renewable generation by 2020. Table 1 shows the growth rate of different clean energy technologies, which indicates a high growth rate in the wind energy as a source of clean energy [4].

1.2. Classification of wind turbines

With the intention of using this abundant source of wind energy, various designs have been proposed till date. Depending on their axis of rotation wind turbines are mainly two types: horizontal axis wind turbine (HAWT) and vertical axis wind turbine (VAWT). HAWTs are very well known for their comparatively higher efficiency over VAWTs and inherently have been used for electricity production. However, the VAWTs have significant advantages over HAWTs because of their lower installation and maintenance costs, lesser wear on the moving parts, and independency on wind direction. Further, these machines do not require any yaw mechanism and over speed control. These advantages make them suitable for small-scale applications [5,6]. Based on the designs, VAWTs can be broadly classified into two categories such as Savonius and Darrieus rotor [7,8]. The Darrieus wind rotors are more efficient then Savonius rotors and are mostly used as a distributed micro-wind power generator. However, at lower wind speed regions, the Savonius rotors have shown a better starting ability than the Darrieus rotors. The applications of Savonius rotor include water pumping, providing ventilation and agitating water to keep stock ponds ice-free during winter, generating micro-wind power for standalone systems and starting torque producer for other VAWTs [6,9,10].

2. Purpose of the present study

Numerical simulation, optimization techniques and soft-computing techniques play a very vital rule to optimize the performance of rotors and finding out the best suitable configuration and control. Although, the experimental studies have shown more accurate findings, however, the computational studies have given the freedom to carry out a large-scale research with lesser experimental hazards and costs. Very recently, Akwa et al. [6] have given an overall idea and useful information on the experimental parameters of Savonius rotors. Till now different CFD methods like finite volume method, finite element method, finite difference method; turbulence models like one equation turbulence model, two-equation and hybrid CFD turbulence models; and soft-computing techniques like artificial neural network (ANN), fuzzy logic and adaptive neuro-fuzzy interface have been used by several researchers for improving the performance of Savonius rotor. Combining all, this review work tries to give a clear idea on different computational methods applied and their capability to predict the flow physics as well as performance of the Savonius rotor.

3. Basic concepts of Savonius rotor

A Finish engineer Savonius [7] introduced the Savonius rotor in 1920s. He has reformed the design of Flettener's rotor [11] by dividing a cylinder into half, along its central axis and relocating the two semi-cylindrical surfaces sideways. This shape is akin to "S" when viewed from top as shown in Fig. 1. These type of rotors may be of two, three or higher bladed systems and can be used in single- or multi-staged arrangements. The working principle is based on the difference of the drag force between the convex and the concave parts of the rotor blades when they rotate around a

Nomenclature

Greek symbols

δ	overlap ratio
ω	specific dissipation rate
ε	energy dissipation rate
θ	rotor blade angle (degree)
α, β	angle of curtain plate (degree)

Notations

AR	aspect ratio
C_P	power coefficient
C_T	torque coefficient
D	rotor diameter (m)
d	chord length of the blade (m)
e	overlap distance between rotor blades (m)
F	blockage correction factor
H	rotor height (m)
k	turbulence kinetic energy (m^2/s^2)
l_1, l_2	length of curtain plate (m)
Re	Reynolds number
u	rotor tip speed (m/s)
V	wind speed (m/s)

vertical shaft. During the complete rotational cycle, various types of flow patterns such as coanda-type, dragging, overlap, stagnation, and vortex flows are observed around the rotor. A detailed description of various rotor arrangements and flow patterns are available in a recent review work of Akwa et al. [6].

Following the work of Savonius [7], Bach [12] has made some investigations in the area of the Savonius rotor and related machines in 1931 and has recorded the highest efficiency of 24%. Thereafter, for over a period of 30 years, studies on Savonius rotor have hardly found its existence. Later, Simonds and Bodek [13], MacPherson [14], and other researchers [15–20] carried out experiments on Savonius rotors and reported a very low efficiency. As a result, there is a need of research to optimize the design and performance of the rotor. On this aspect, Wilson et al. [21], and Van Dusen and Kirchhoff [22] initiated the computational studies on Savonius rotors in 1970s. Subsequently, several other researchers have carried out numerical studies on Savonius rotors [10,23–31]. The following sections give a detailed review of computational work in the area of Savonius wind rotor.

4. Application of CFD methodology on Savonius rotor

Computational fluid dynamics (CFD) is a very powerful tool to solve a wide range of industrial and non-industrial fluid flow problems. Physical characteristics of the fluid motion around the rotor could be described through the fundamental flow governing equations, usually in the partial differential forms. In order to analyze the governing equations, high level computer programming

Table 1
Recent deployment growth compared with clean energy targets [4].

Technology	Current rate (%)	Required annual growth to 2020 (%)	Current status (GW)	Blue map target 2020 (GW)
Biofuel	18	7	2.54 (EJ)	5.04 (EJ)
Biomass	7	4	54	82
Hydropower	5	2	980	1219
Solar PV	60	19	21	126
Wind power	27	12	195	575
Energy intensity of manufacturing	−1.30	−0.60	3.73 (MJ)	3.81 (MJ)
Geothermal power	4	7	11	21
Nuclear power	3	4	430	512
CSP	8	50	0.6	42
Electricity generation with CCS	Zero projects	3 (GW per year)	Zero projects	28

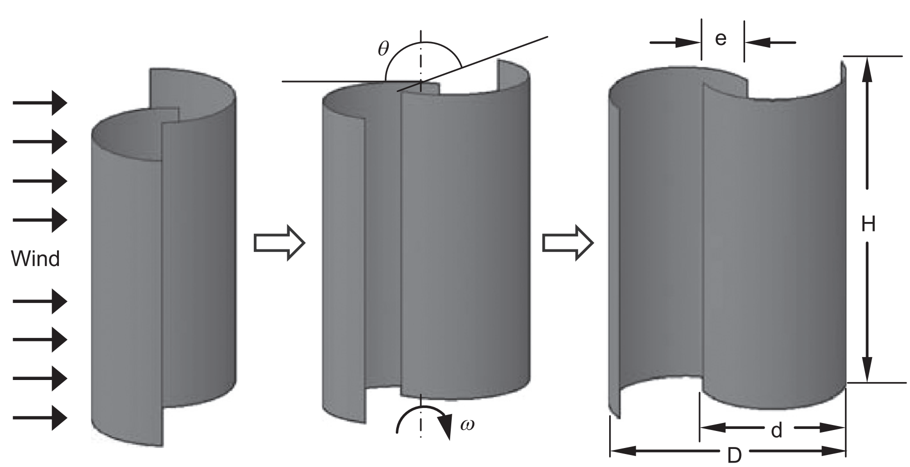


Fig. 1. Schematic diagram of a two-bladed Savonius rotor at different angular positions.

languages like C, Fortran or software packages like ANSYS, ADINA, STAR-CD, COSMOS-Floworks etc. have been used [32].

All the codes and software for solving the flow governing equations around a rotor involves three main elements (i) a preprocessor, (ii) a solver, and (iii) a post processor. Preprocessing stage involves (a) specification of the computational domain around the rotor, (b) modeling of the rotor geometry, (c) grid generation and meshing, (d) definition of flow properties and (e) specifying the boundary conditions. Following the preprocessing stage, three types of discretization solvers have been used, viz., finite difference method (FDM), finite volume method (FVM) and finite element method (FEM). This solver stage involves (i) approximation of the unknown flow variables, (ii) discretization by substitution of the approximations into the governing flow equations and subsequent mathematical manipulations and (iii) solution of the algebraic equations. The post-processing stage, thereafter, involves the visualization of the results like (i) domain geometry and grid display, (ii) vector plots, (iii) contour plots, (iv) 2D and 3D surface plots, (v) force monitors, and (vi) translational and rotational views etc. Besides all these, the grid and domain independence tests for a particular rotor analysis are also important. All the solving methods have merits as well as demerits based upon the assumptions made and methodologies applied. Some of these are discussed in the following sections.

4.1. Use of finite difference method (FDM)

The first step of FDM toward obtaining a numerical solution involves the discretization of the geometric domain. Truncated Taylor series expansions are often used to generate finite difference approximations of property derivatives at each grid point and its neighbours. These are replaced by finite differences yielding an algebraic equation for the values of the property at each grid point. Kawamura and Sato [29] studied this concept of solving the flow around the wind rotor. Boundary fitted coordinate system was used to state the blade shape and the rotating coordinate system was on the rotor blades for desired rotation. The derived equations were solved using finite difference method. A third order upwind discretization scheme was used to treat the nonlinear terms of Navier–Stokes (N–S) equations. Other spatial derivatives were solved by central difference scheme. Torque value was determined from the pressure data on either side of the blades.

4.2. Use of finite volume method (FVM)

Fundamentally, the finite volume method is originated from the special finite difference formulation. It is the formal integration of the governing equations of the fluid flow over all the (finite) control volumes of the computational domain. This is followed by discretization of the terms in the integrated equation representing the flow over the Savonius rotor. This converts the integral equations into a system of algebraic equations. Finally, the algebraic equations are solved by different iterative methods. ANSYS-Fluent and ANSYS-CFX are the widely accepted finite volume software packages to solve complex flow phenomena [30,33–43]. Investigations have also been carried out with the help of ANSYS-CFX package for analyzing the performance of Savonius rotor [44,45]. Apart from these software packages, mathematical models using different programming languages based on the finite volume method have been developed [46].

4.3. Use of finite element method (FEM)

The finite element method uses simple piecewise functions (e.g., linear or quadratic) valid on elements to describe the local variations of unknown flow variables around the Savonius rotor. The governing equations are precisely satisfied by the exact solutions of the unknown variables. If the piecewise approximating functions for unknown variables are substituted into the equation, it does not hold exactly and a residual is defined to measure the errors. Thereafter, the residuals (and hence the errors) are minimized in some sense by multiplying them by a set of weighting functions and integration. As a result, a set of algebraic equations are obtained for the coefficients of the approximating functions. Finally, the set of algebraic equations are solved by using various iterative methods. Two different finite element based software packages viz., COSMOS-floworks and ADINA (Automatic dynamic incremental non-linear analysis) have been reported in the literature for solving the fluid flow problems around a Savonius rotor [31,47].

4.4. Use of special methods

4.4.1. Discrete vortex method (DVM)

In discrete vortex method, the flow is considered to be imbedded with a finite number of discrete vortices. When the flow passes over a rotor body, the flow splits at the sharp edges and the shear layers are shedded downstream from the separation points where the nascent free vortices are formed [25]. To obtain the pressure distribution, the velocities on either side of blades are calculated assuming a uniformly distributed vorticity over the length of the element. The pressure coefficient is then obtained by solving the unsteady Bernoulli equation [24]. Wilson et al. [21] had first applied the discrete vortex theory in the field of Savonius rotor. Following them, Van Dusen and Kirchhoff [22] developed another model using vortex shedding. However, an attached flow was assumed in both the analyses that made the solutions unrealistic. However, Ogawa [23] gave a more qualitative results rather than quantitative results when he used the DVM by assuming flow separation at the tips of the blades. Modeling of flow separation showed a great potential for implementation of discrete vortex method for analyzing the flow over Savonius rotor [23–27,48]. Based on a 2D unsteady DVM formulation, a FORTRAN code was developed to find the torque distribution of the stationary rotor and the unsteady pressure field on the rotating rotor blades that showed a good agreement with the experimental data only at low *TSRs* [48,49].

4.4.2. Domain decomposition method (DDM)

In domain decomposition method, as reported by Kawamura et al. [28], the rotor computational domain was divided into two sub-domains, where one included the rotor with two semi-circular regions, while the other, a rectangular region, included the fixed walls. Both the domains had a common overlapping region.

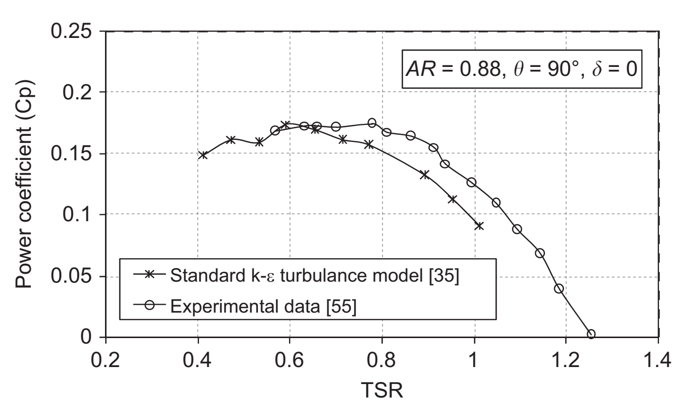


Fig. 2. Comparison of standard k–ε turbulence model results with experimental data [35,55].

Rotational coordinate system was used for the rotor domain, whereas cartesian coordinate system was used for the fixed wall domain. The boundary values were calculated from the grid point values of another domain through the interpolation. The incompressible N–S equation was solved by the standard marker-and-cell (MAC) method. For numerical stability, the non-linear terms of the governing equations were treated with third order upwind scheme. All other spatial derivatives were treated with second order central difference scheme. Euler explicit scheme was used for the time integration. This method had shown its ability for parallel computation and saved a large amount of computational time [28].

5. Selection of the turbulence models for rotor simulation

The flow field around a Savonius rotor is turbulent in nature. Thus, while selecting a suitable numerical approach, the features of turbulence must be considered for obtaining the desired results. However, each of the turbulence models has their own merits and demerits. The various types of turbulence models that have been used so far are discussed briefly in the following section.

Among the various turbulence models, the Spalart–Allmaras (SA) model is a simple one-equation turbulence model, where the near wall gradients of the transported variable are much smaller than the turbulent kinetic energy equation based (k–ε) models. This might made this model less sensitive in the near walls treatment around the Savonius rotor. However, a 3D CFD simulation using SA model was carried out to compare the performance of vertical-axis spiral rotor with two end plates and one middle plate with a conventional Savonius rotor. Results of the simulation depicted that torque performance of the spiral rotor was more favorable during its whole rotation cycle [50]. The standard k–ε model [51] is the basic k–ε turbulence model and more suitable when flow is fully turbulent and has given better results than SA model for turbine analysis [52]. Two-dimensional steady computational studies were subsequently carried out for Savonius rotor and for combined Savonius–Darrieus rotor. However, due to high unsteadiness and two-dimensional assumption, the computational results have not guaranteed the accuracy of the standard k–ε model [38,53,54]. Using the standard k–ε turbulence model, a 3D study was made on a helical Savonius rotor and the results obtained [35] had shown a general agreement with the experimental data [55] as shown in Fig. 2. Renormalization of the k–ε model gives an additional term in the ε-equation and significantly improved the accuracy for swirl flows, which is well known as RNG k–ε turbulence model. The prediction ability of the RNG model is also observed in the studies of Yonghai et al. [36] and Emmanuel and Jun [56]. In another study using RNG k–ε turbulence model, it is observed that 2D simulation has over predicted the rotor performance, whereas 3D simulation has shown more accurate predictions as shown in Fig. 3 [37]. The realizable k–ε model gives a new formulation for turbulent viscosity and dissipation rate and is comparatively newer from the other k–ε turbulence models. As seen from the reported investigations, both the realizable and RNG k–ε models have found to be significantly improved models over the standard k–ε and SA models [57].

The shear stress transport (SST) k–ω turbulence model is a two-equation eddy viscosity model combining the advantages of both k–ε formulation for free stream flow and k–ω formulations in the rotor boundary layer [58,59]. Using this model in CFX 12.0 software, Abraham et al. [45] have carried out a two-dimensional study on the Savonius rotors. Although there seems to be a general agreement between computational and experimental data, however, the 2D simulation results are over predicting the experimental data (Fig. 4). Further, using three-dimensional SST k–ω turbulence model, a very good agreement with the experimental results is found in the work of Plourde et al. [60]. Considering the practical flow phenomena with high unsteady property and massive flow separation, Spalart and his coworkers [61] have suggested the Detached-Eddy Simulation (DES). The objective was to develop a numerically feasible and accurate approach through merging the most favorable features of RANS models and Large Eddy Simulation (LES). A comparative study of 2D k–ω SST, 3D k–ω SST, and Hybrid Detached-Eddy Simulation (DES) k–ω SST turbulence model was carried out to analyze the flow filed behavior and wake geometry of a two bladed Savonius rotor [43]. It is perceived that 2D k–ω SST turbulence model was over predicting, whereas 3D k–ω SST turbulence model was slightly under-predicting the experimental results. The hybrid 3D DES/ k–ω SST turbulence model, on the other hand, gave a more accurate prediction as shown in Fig. 5 [43].

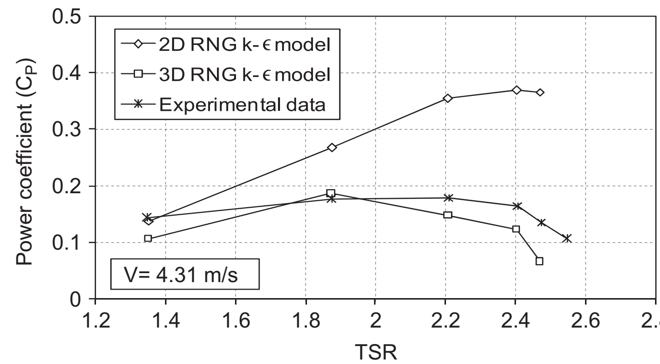


Fig. 3. Comparative analysis of 2D and 3D RNG k–ε model results with experimental data [37].

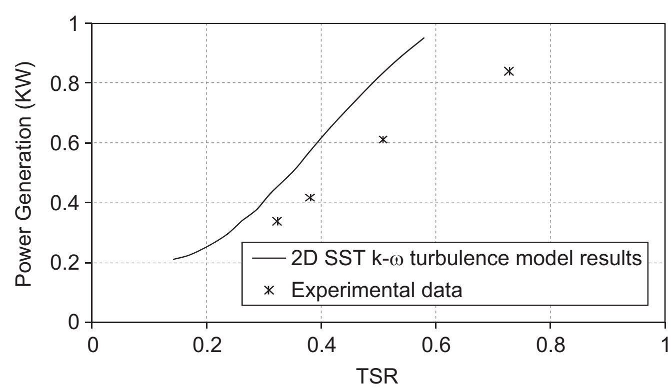


Fig. 4. Comparison of 2D SST k–ω turbulence model results with experimental data [45].

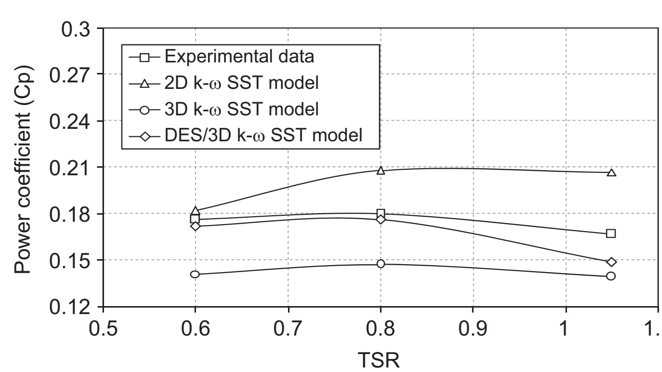


Fig. 5. Comparison of different turbulence models with experimental data [43].

6. Application of soft-computing techniques on Savonius rotor

During last 25 years, apart from CFD, various soft-computing techniques like fuzzy logic, artificial neural networks (ANN) and genetic algorithms have shown significant ability for prediction of power factor of several energy systems such as in solar radiation, wind speed prediction, photovoltaic system, building services systems and load forecasting [62]. Through ANN study, Sargolzaei [63] predicted the power ratio for Savonius rotors of six different blade shapes at various Reynolds number. The results showed a reasonable agreement with the experimental results for maximizing the power and efficiency of the rotor. The proposed method of parallel information processing and generalization of ANN also have shown high computational speed. Again, using Radial Basis Function (RBF) network, an ANN study was carried out to predict the power and torque output as a function of tip speed ratio for various rotor shapes. An admirable agreement was observed between the experimental results and ANN prediction [64]. Further research on adaptive neuro-fuzzy inference system (ANFIS) was carried out to find out the effectiveness of ANFIS over fuzzy inference system (FIS) and RBF-ANN. Fig. 6 shows a comparative study of these approaches, which clearly indicates the advantages of ANFIS over other methods [65].

7. CFD analysis on the influencing parameters

The performance of the Savonius rotor is often expressed in terms of power coefficient (C_P) and torque coefficient (C_T). These aerodynamic coefficients heavily depend on the various the designing parameters of the rotor. Akwa et al. [6] reported a detailed description on the various design arrangements and parameters of the rotor. Although Savonius rotor has some significant advantages, a simple Savonius rotor bids a very low C_P of around 0.15, whereas a HAWT and Darrieus type rotor give C_P of 0.45 and 0.35, respectively [66]. In keeping with the demand, computational studies have been carried out for last 30–40 years along with the experiments to improve the efficiency of the Savonius rotor. In another study, the C_P of a conventional Savonius rotor with two- and three-bladed systems are found to be 0.18 and 0.15, respectively. The C_T, on the other hand, are found to be 0.33 and 0.35 for two- and three-bladed rotors, respectively [40]. Through optimization of the influencing parameters like tip speed ratio, overall ratio, aspect ratio, blade shape and rotor angle, the rotor performance is increased significantly, and these features are discussed in the subsequent sections.

7.1. Tip speed ratio (TSR)

Tip speed ratio (*TSR*) is defined as ratio of rotor tip speed (u) to the free wind speed (V). Using 2D simulation in the FVM based Fluent software, Kianifar and Anbarsooz [67] have predicted that the highest C_P is obtained in the range of *TSR* between 0.8 and 1.0. This has shown a good agreement with the results of Hayashi et al. [33], although there are several studies on the effect of *TSR* as shown in Table 2 [24,35,38,40,41,43]. Using a 2D discrete vortex method, it was reported that the optimum performance for Savonius rotor was obtained at *TSR* of 1.2 and a reasonable agreement was achieved with experimental data [24]. Again, using DVM, a developed FORTRAN code effectively predicted the rotor

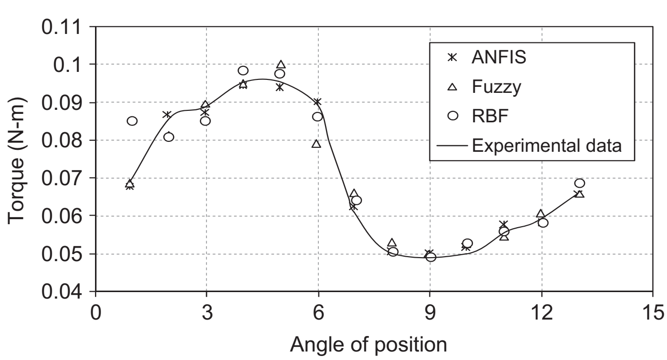


Fig. 6. Comparison of ANFIS, Fuzzy, and RBF model results with experimental data [65].

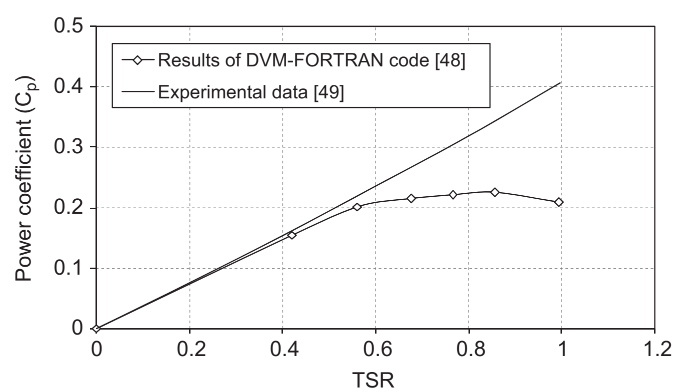


Fig. 7. Comparative analysis of DVM-FORTRAN code with experimental data [48,49].

Table 2
Comparison of different influencing parameters from the available literature.

Influencing parameter	Researcher(s)	CFD methodology	No. of blades	Optimum performance value
Tip speed ratio (*TSR*)	Modi and Fernando [24]	2D discrete vortex formulation	2	1.2
	Dobrev and Massouh [43]	FVM with 3D DES/k–ω SST model	2	0.8
		2D k–ω SST model	2	
		3D k–ω SST model	2	
	Zhao et al. [35]	FVM with 3D standard k–ε model	2	0.81
			3	0.55
	Kianifar and Anbarsooz [67]	FVM with 2D standard k–ε model	2	0.8 to 1.2
	Mahamed et al. [40]	FVM with 2D realizable k–ε model	2	0.7
			3	0.8 (with shielding)
Aspect ratio (*AR*)	Zhao et al. [35]	FVM with 3D standard k–ε model	2	6.0
Overlap ratio (δ)	Debnath et al. [38]	FVM with 2D standard k–ε model	3	0.2
	Kianifar and Anbarsooz [67]	FVM with 2D standard k–ε model	2	0.2
	Menet and Bourabaa [30]	FVM 2D two-equation model	2	0.242
	Yaakob et al. [47]	FEM 3D model	2	0.21
Rotor angle (θ)	Altan and Atilgan [34]	FVM with 2D standard k–ε model	2	45°
	Zullah et al. [44]	FVM with 2D standard k–ε model	3	40°

performance up to $TSR = 0.6$ as shown in Fig. 7 [48]. Alternatively, for a helical Savonius rotor, the highest power coefficients are obtained at $TSR = 0.81$ and 0.55 for two- and three-bladed rotor, respectively [35]. Fig. 8 shows a good agreement of using a suitable *TSR* of 0.7 for a two-bladed Savonius rotor [33,40].

7.2. Aspect ratio (AR)

Aspect ratio (*AR*) is defined as the ratio of height (*H*) of the rotor to its diameter (*D*) as shown in Fig. 1. A high *AR* of the rotor improves the efficiency, but most of the existing rotors are found to have low *AR* because of structural reasons. However, it is possible to improve the efficiency using end plates in a low aspect ratio bladed rotor. With a larger rotor diameter, higher torque will be achieved but the rotational speed will be reduced and vice versa [68]. Thus, present situation demands the need of an optimum *AR*. A 3D computational study reported a comparative analysis among different *ARs* (Fig. 9) and depicted a better performance with a high *AR* of 6.0 for two-bladed helical rotors [35].

7.3. Overlap ratio (δ)

Overlap ratio plays a very vital role in optimizing the performance of Savonius rotor and is defined as the ratio of the overlap distance between two blades (*e*) to the chord length of the blade (*d*) as shown in Fig. 1. With the help of a finite element based software COSMOS-Floworks, the effect of overlap ratios has been studied. This study has shown a maximum torque (Fig. 10) at an optimum δ of 0.21 [47]. These results also confirm a good agreement with the experimental investigations of Menet [10] and Gupta et al. [69]. For a combined 2D Savonius–Darrieus rotor, a computational study reported an optimum δ of 0.2 [38]. For helical Savonius rotors, the optimum δ is obtained at 0.3 [35]. The static simulation studies of Menet and Bourabaa [30] have reported an optimum δ of 0.242. Recently, Kianifar and Anbarsooz [67] reported an increase in power coefficient when δ increases from 0 to 0.2, and beyond which the power coefficient decreases [67]. The above observations indicated an optimum overlap ratio in the range of 0.2–0.25.

7.4. Rotor angle (θ)

The rotor static torque values greatly depend on the rotor angle. It is the angle between the chord of the rotor blade to the direction of wind flow (Fig. 1). The static torque variation with different rotor angles is shown in Fig.11. It demonstrates that at $\theta = 45^\circ$, the rotor static torque value is highest [34]. The CFX simulations carried out with two different rotor angles of 40° and 60° reported a higher efficiency and a better self-starting capability of the rotor at $\theta = 40^\circ$, [44]. Thus, it is apparent that the highest static torque value lies in the range of $\theta = 40$–45°.

7.5. Reynolds number (Re)

It is an important non-dimensional parameter for defining the flow characteristics around a wind rotor. According to Akwa et al. [6], this parameter plays a significant role on the flow separation and boundary layer formation around the rotor blades. Simulation studies have reported that the static torque coefficient increases from 0.09 to 0.22 as the *Re* increases from 0.4×10^5 to 8.67×10^5 [6]. Moreover, the performance of a Savonius rotor also increases with the increase in Reynolds number. It was reported that the highest C_P was increased from 15.2% at $Re = 0.8 \times 10^5$ to 17.5% at $Re = 1.5 \times 10^5$ [30,70].

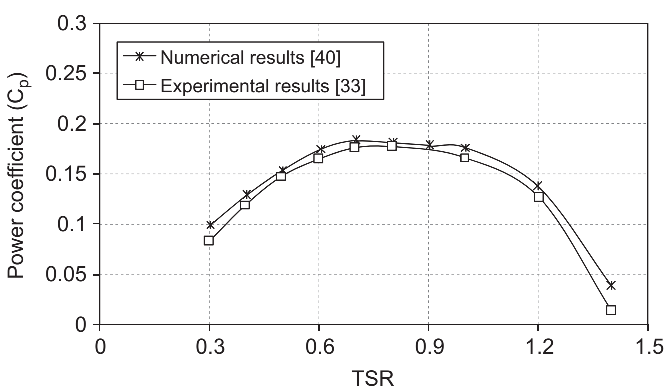


Fig. 8. Effect of *TSR* on the power coefficient of Savonius rotor [33,40].

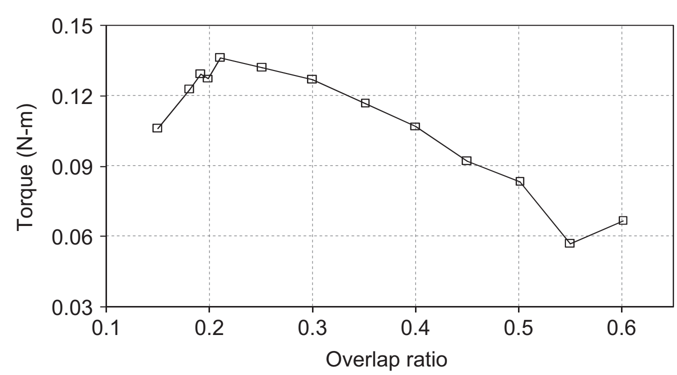


Fig. 10. Torque variation for different overlap ratios [47].

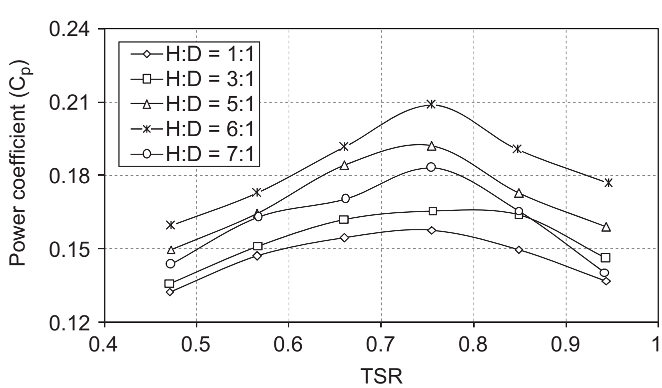


Fig. 9. The effect of aspect ratio on the power coefficient of Savonius rotor [35].

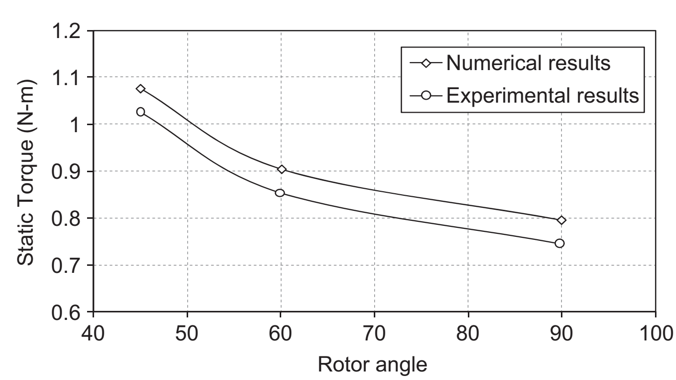


Fig. 11. Effect of rotor angular position on the static torque performance [34].

7.6. Blockage factor (F)

Wind tunnel data presented by different investigators often cannot be correlated due to varying test conditions. One of the major parameters affecting the test data is the blockage. It is an important parameter to be taken into account while comparing the wind tunnel results with those obtained outside the wind tunnel [45]. The blockage correction factor (F) is determined by

$$F = \frac{\text{Power}_{rotor}}{\text{Power}_{free}} \tag{1}$$

The value of F is approximately taken as 2, which can be reinforced, by taking wind power scales with the cube of wind velocity. Assuming 25% higher velocity at the tunnel condition, the blockage factor can be determined by

$$F \sim \left(\frac{V_{tunnel}}{V_{free}}\right)^3 = 1.25^3 = 1.95 \tag{2}$$

Abraham et al. [45] reported the blockage factor in respect of simulated torque as given below:

$$F = \frac{\text{Torque}_{tunnel}}{\text{Torque}_{free}} = 1.85 \tag{3}$$

The results obtained from power approximation, wind speed scale and simulated torque gave a good agreement of blockage factor [45].

7.7. Number of blades

The number of rotor blades is an effective parameter depending upon the operating conditions. Normally two, three, and four-bladed rotors have been used. Two-bladed rotor has shown a better performance over three- and four-bladed rotors, although the starting static torque is higher in case of three-bladed rotor. However, four-bladed rotor has shown a much lesser efficiency as compared to two-bladed rotor [16]. A numerical study to optimize the number of blades had shown the C_P to be 0.165 and 0.12 for two- and three-bladed rotor, respectively [35]. The observations of this study matches with the work of Saha et al. [71]. In a study, using OPAL-CFD, the two-bladed rotor has shown a highest C_P of 0.2503 as compared to 0.2120 for a three-bladed rotor [41]. However, in a recent work, a six-bladed rotor seemed to have shown a highest power coefficient of 0.3, which is higher than a standard two-bladed rotor [56].

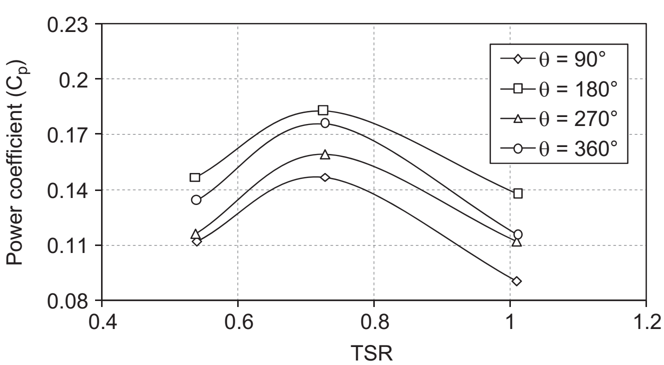


Fig. 12. The effect of helical angle on the power coefficient of Savonius rotor [35].

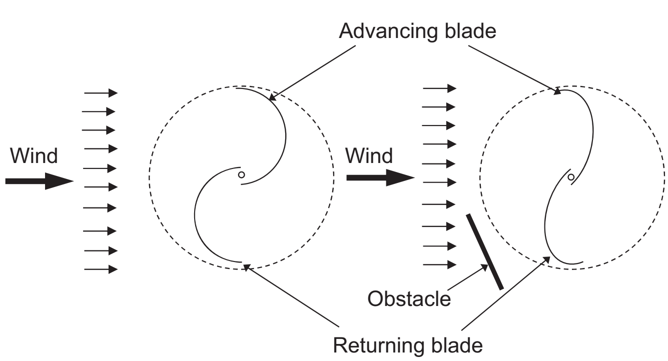


Fig. 13. Optimum configuration (right) compared to the conventional Savonius turbine [41].

7.8. Blade shape

A helical blade shape of Savonius rotor was studied numerically with k–ε turbulence model for various angles of twist. Fig. 12 shows a comparative analysis for different twist angles for two-bladed Savonius rotor, where a best rotor performance is observed at a twist angle of 180°. Implementation of this helical shape improves the rotor performance from 0.15 up to 0.2 without any additional equipment [35]. Again, a two-bladed spiral Savonius rotor with end plates has shown better and steadier torque performance than conventional Savonius rotor [50]. Using OPAL-CFD package, the blade shape of the Savonius rotors was modified through optimization algorithms as shown in Fig. 13 and reported a high C_P of 0.298 [41]. These results encourage further need of research on the shape of Savonius rotor. Table 2 shows the comparison of different influencing parameters and their effects on the performance of Savonius rotor based on the available computational literature. From this Table, a better conclusion can be drawn for different influencing parameters and CFD methods.

8. CFD analysis on the augmentation techniques

The performance of Savonius rotor can be improved by introducing various augmentation techniques like multi-stages rotor, curtain design, windshields, and convergent nozzle in the wind energy conversion system. Numerical studies on the augmentation techniques are scarce; however, an attempt has been made to discuss them briefly in the following sections.

8.1. Use of multi-staging

Multi-staging is usually done to improve the self-starting capability of a Savonius rotor. In these type of arrangements, the rotor blades are set at 90° and 120° to each other for a double-stage and three-stage rotor assembly, respectively [10,33]. Very few numerical investigations in this area are found in open literature [45,47]. In some instances, Savonius rotor and straight bladed Darrieus turbine are multi-staged together to enhance the starting ability and performance of the system. Using a finite volume based mathematical model, the static torque co-efficient of this type of combined Savonius–Darrieus turbine is found to be 10 times better than the conventional straight bladed Darrieus turbine [46]. Further, at higher rotational speeds ($TSR > 1.8$), the dynamic torque co-efficient of this combined system is considerably improved than simple straight-bladed turbine.

8.2. Use of curtain design

The uses of curtains significantly enhance the static torque and dynamic characteristics of a Savonius rotor. The curtains, placed at the front side of the rotor, are used to prevent the negative torque on the convex side of rotor blade (Fig. 14). Using standard k–ε turbulence model, a CFD study was carried out with on different rotor positions ($\theta = 45°$, 60° and 90°) and at different curtain angles ($\alpha = 30°$–60° and $\beta = 10°$–15°). It is observed that the curtain 1 with

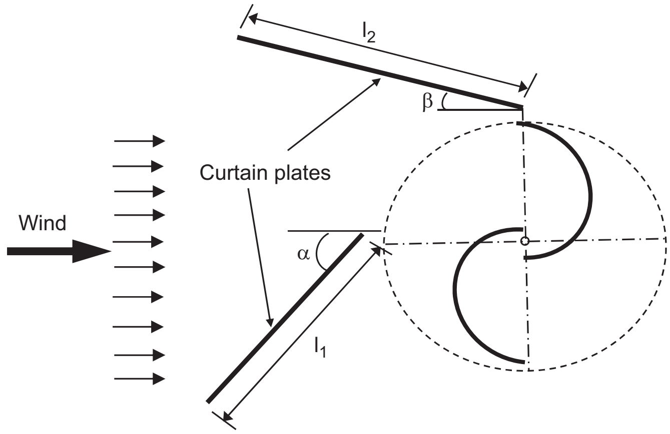


Fig. 14. Design of the curtain arrangement [34].

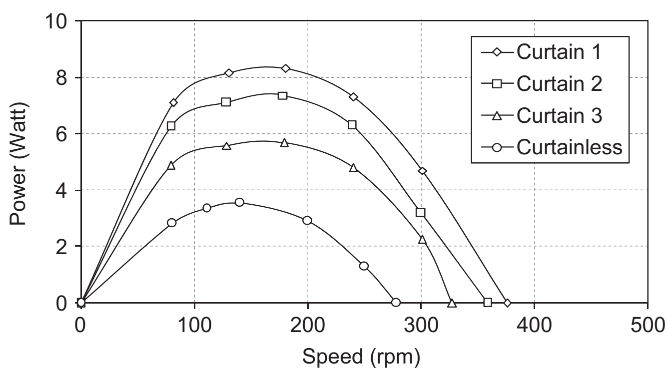


Fig. 15. Comparison of the power changes with the rotor with and without curtain designs [39].

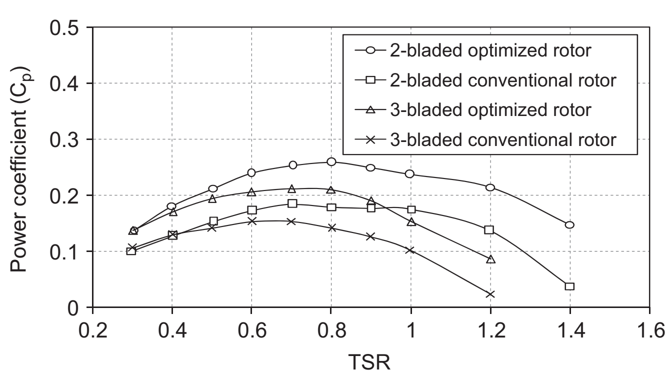


Fig. 16. Performance comparison between the optimized configuration and the conventional 2- and 3-bladed Savonius rotors [40].

l_1=45 cm and l_2=52 cm, when placed with α=45° and β=15° has given a better static torque and highest C_P of 0.38 as shown in Fig. 15 [34,39].

8.3. Use of wind shields

The shielding on the returning blade can be a viable option to cut the wind pressure inserted to the returning blade (Fig. 13). A DVM based numerical study was made to predict the flow flied around a Savonius rotor with windshield [26]. Another study, using RNG k–ε turbulence model, depicted a much reduced negative torque, and hence, an increase in the mean torque from 11.8 N-m to 24.23 N-m with a windshield placed at an angular position of 30° [36]. In order to locate a suitable position of obstacle windshields, Mohamed et al. [40] used an optimization package OPAL-CFD, where they found a highest C_P of 0.25 and 0.21 for two- and three-bladed rotors, respectively (Fig. 16).

8.4. Use of convergent nozzle

In order to cut the negative torque, another possible option is to use a convergent nozzle at the front of the rotor. The nozzle in this case performs two functions viz., (a) it amplifies the effective wind speed on the rotor and (b) it prevents the negative torque [72]. At present, the shortage of available literature is demanding the need of computational research on the effectiveness of convergent nozzle.

9. Conclusions

It is seen that the effectiveness of performance prediction of Savonius rotor depends upon the flow assumptions in the computational methodology as well as choice of the discretization methods and solution models. The performance of the Savonius rotor mainly depends upon various parameters such as tip speed ratio, overlap ratio, aspect ratio, blade angle, blade shape, and number of blades. Moreover, the performance can also be improved by introducing various augmentation techniques such as curtain design, obstacle shielding, multi-staging, and nozzles. Over the last few decades, a number of numerical investigations in the area of Savonius rotor have been carried out, and based on their studies, some of the salient points are summarized below.

9.1. Flow assumptions and computational methodology

- Flow around the Savonius rotor is fully turbulent and unsteady in nature. Flow separation and vortex shedding are the common phenomenon around this rotor due to its working nature and continuous variation in the flow angle with respect to blades.
- The hybrid DES/k–ω SST turbulence model has shown the benefits of capturing the unsteady effects more precisely. However, 3D k–ω SST turbulence model also shown a close prediction capability of the rotor performance.
- The 2D computational study always over-predicts the performance, whereas the 3D study shows a better prediction capability.
- The finite volume method appears to be superior as compared to finite difference and finite element methods in solving the complex flow phenomena over the Savonius rotor.
- The ANFIS has shown a promising methodology for predicting the power output of Savonius rotor over other methods of soft-computing technique such as FIS and RBF-ANN.

9.2. Influencing parameters and augmentation techniques

- For two- and three-bladed conventional rotor, the power coefficient (C_P) values are of the order of 0.18 and 0.15, respectively. The torque coefficient (C_T) values, on the other hand, are found to be around 0.33 and 0.35, respectively.
- The highest C_P is obtained in the range of TSR=0.7 to 1.2 and in the range of δ=0.2 to 0.25. The highest static torque value of Savonius rotor is achieved in the range of θ=40–45°.
- Blockage correction factor of around 2 has to be taken into account when comparing the wind tunnel data with the actual field data.
- Helical as well as spiral shapes with different twisting angle have shown significant improvement on the performance of Savonius rotor.

- Multi-staging of rotor increases the starting torque of the rotor. The curtain designs with optimum length and position significantly increases the C_P up to 0.38. The negative torque can be significantly reduced by suitably positioning the wind-shields at the front of the rotor.

From the above discussions, it is observed that using an appropriate computational methodology, the power output as well as starting ability of the Savonius rotor can be optimized. Although, till date, the influencing parameters are optimized in some extent, however, they have not been optimized to a precise value through extensive numerical investigations. In view of this, there is a necessity of further numerical investigation on different turbulence models and soft-computing techniques to predict the rotor performance characteristics more precisely.

References

[1] Boyle G. Renewable energy: power for a sustainable future. New York: Oxford University Press; 978-0-19-958651-6.

[2] Burton T, Sharpe D, Jenkins N, Bossanyi E. Wind energy handbook. UK: John Wiley & Sons Limited; 0-471-48997-2.

[3] Manwell JF, Mcgowan JG, Rogers AL. Wind energy explained: theory, design and application. UK: John Wiley & Sons Limited; 978-0-470-01500-1.

[4] International Energy Agency (IEA). Clean energy progress report-2011. 1–67 June.

[5] Tabassum SA, Probert SD. Vertical-axis wind turbine: a modified design. Applied Energy 1987;28(1):59–67.

[6] Akwa JV, Vielmo HA, Petry AP. A review on the performance of Savonius wind turbines. Renewable and Sustainable Energy Reviews 2012;16(5):3054–64.

[7] Savonius SJ. The S-rotor and its applications. Mechanical Engineering 1931;53 (5):333–8.

[8] Darrieus GJM.. Turbine having its rotating shaft transverse to the flow of the current. US patent publication: Publication No. US-1835018; 1931.

[9] Fujisawa N, Gotoh F. Pressure measurements and flow visualization study of a Savonius rotor. Journal of Wind Engineering and Industrial Aerodynamics 1992;39(1–3):51–60.

[10] Menet JL. A double strap Savonius rotor for local production of electricity: a design study. Renewable Energy 2004;29(11):1843–62.

[11] Flettner A. The story of the rotor. London: Crosby Lockwood; 1926 OCLC: 277536025.

[12] Bach G. Investigations concerning Savonius rotors and related turbomachines. Translated into English by Brace Research Institute, Quebec, Canada 1964; Forschungauf Gebiete des Ingenieurwesens 1931;2(6):218–23.

[13] Simonds MH, Bodek A. Performance tests of a Savonius rotor. Brace Research Institute, McDonald College of McGill University, Quebec, Canada. 1964 Report no-T10.

[14] Macpherson RB. Design, development and testing of low head high efficiency kinetic energy machine. MTech Dissertation. University of Massachusetts, Amherst, United States; 1972.

[15] Newman BG. Measurements on a Savonius rotor with variable air gap. M.Tech Dissertation. McGill University, Canada; 1974.

[16] Sheldahl RE, Feltz LV, Blackwell BF. Wind tunnel performance data for two- and three-bucket Savonius rotors. AIAA Journal of Energy 1978;2(3):160–4.

[17] Sivasegaram S. Secondary parameters affecting the performance of resistance type vertical axis wind rotors. Wind Engineering 1978;2(1):49–58.

[18] Suzuki T, Okitsu H. Characteristics of a Savonius windmill power system with a synchronous generator. Wind Engineering 1982;6(3):131–9.

[19] Modi VJ, Roth NJ. Fernando MSUK. Optimum-configuration studies and prototype design of a wind-energy-operated irrigation system. Journal of Wind Engineering and Industrial Aerodynamics 1984;16(1):85–96.

[20] Mojola OO. On the aerodynamic design of the Savonius wind mill rotor. Journal of Wind Engineering and Industrial Aerodynamics 1985;21(2):223–31.

[21] Wilson RE, Lissaman PBS, Walker SN. Aerodynamic performance of wind turbines. ERDA/NSF/04014-7611 1976:111–64.

[22] Van Dusen ES, Kirchhoff RH. A two dimensional vortex sheet model of a Savonius rotor. Fluid engineering in advanced energy systems. In: Proceedings of the ASME winter annual meeting; San Francisco, California; December 10–15 1978:15–31.

[23] Ogawa T. Theoretical study on the flow about Savonius rotor. ASME Transactions: Journal of Fluids Engineering 1984;106(1):85–91.

[24] Modi VJ, Fernando MSUK. Unsteady aerodynamics and wake of the Savonius wind turbine: a numerical study. Journal of Wind Engineering and Industrial Aerodynamics 1993;46-47:811–6.

[25] Fernando MSUK VJ. A numerical analysis of the unsteady flow past a Savonius wind turbine. Journal of Wind Engineering and Industrial Aerodynamics 1989;32(3):303–27.

[26] Kotb MA, Aldoss TK. Flow field around a partially-blocked Savonius rotor. Applied Energy 1991;38(2):117–32.

[27] Fujisawa N. Velocity measurements and numerical calculations of flow fields in and around Savonius rotors. Journal of Wind Engineering and Industrial Aerodynamics 1996;59(1):39–50.

[28] Kawamura T, Hayashi T, Miyashita K. Application of the domain decomposition method to the flow around the Savonius rotor. In: Proceedings of 12th international conference on domain decomposition methods, Chiba, Japan; 25–29 October 1999.

[29] Kawamura T, Sato Y. Numerical simulation of the flow around across-flow wind turbine. Research Institute of Mathematical Science, Kyoto University, Japan 2002;1288(5):44–51.

[30] Menet JL, Bourabaa N. Increase in the Savonius rotors efficiency via a parametric investigation. In: Proceedings of the European wind energy conference & exhibition; London, UK; 22–25 November 2004.

[31] Saha UK, Rajkumar MJ, Maity D. Simulation of flow around and behind a Savonius rotor. International Energy Journal 2005;6(2):83–90.

[32] Tu J, Yeoh GH, Liu C. Computational fluid dynamics: a practical approach. India: Elsevier India Private Limited; 978-81-312-1685-9.

[33] Hayashi T, Li Y, Hara Y, Suzuki K. Wind tunnel tests on a three-stage out-phase Savonius rotor. JSME International Journal Series B: Special Issue on Experimental Mechanics in Heat and Fluid Flow 2005;48(1):9–16.

[34] Altan BD, Atilgan M. An experimental and numerical study on the improvement of the performance of Savonius wind rotor. Energy Conversion and Management 2008;49(12):3425–32.

[35] Zhao Z, Zheng Y, Xu X, Liu W, Hu G. Research on the improvement of the performance of Savonius rotor based on numerical study. In: Proceedings of the IEEE international conference of sustainable power generation and supply (SUPERGEN'09); Nanjing, China; 6–7 April 2009.

[36] Yonghai H, Zhengmin T, Shanshan W. A new type of VAWT and blade optimization. In: Proceedings of the IEEE international conference on technology and innovation-2009 (ITIC). Xian, China; 12–14 October 2009.

[37] Howell R, Qin N, Edwards J, Durrani N. Wind tunnel and numerical study of a small vertical axis wind turbine. Renewable Energy 2010;35(2):412–22.

[38] Debnath BK, Biswas A, Gupta R. Computational fluid dynamics analysis of a combined three- bucket Savonius & three-bladed Darrieus rotor at various overlap conditions. Journal of Renewable and Sustainable Energy 2009;1 (3):1–13.

[39] Altan BD, Atilgan M. The use of a curtain design to increase the performance level of a Savonius wind rotors. Renewable Energy 2010;35(4):821–9.

[40] Mohamed MH, Janiga G, Pap E, Thevenin D. Optimization of Savonius turbines using an obstacle shielding the returning blade. Renewable Energy 2010;35 (11):2618–26.

[41] Mohamed MH, Janiga G, Pap E, Thevenin D. Optimal blade shape of a modified Savonius turbine using an obstacle shielding the returning blade. Energy Conversion and Management 2011;52(1):236–42.

[42] Pope K, Dincer I, Naterer GF. Energy and exergy efficiency comparison of horizontal and vertical axis wind turbines. Renewable Energy 2010;35 (9):2102–13.

[43] Dobrev I, Massouh F. CFD and PIV investigation of unsteady flow through Savonius wind turbine. Energy Procedia 2011;6:711–20.

[44] Zullah MA, Prasad D, Ahmed MR, Lee YH. Performance analysis of a wave energy converter using numerical simulation technique. Science China: Technological Sciences January 2010;53(1):13–8.

[45] Abraham JP, Mowry GS, Plourde BP, Sparrow EM, Minkowycz WJ. Numerical simulation of fluid flow around a vertical-axis turbine. Journal of Renewable and Sustainable Energy 2011;3(3):1–13.

[46] Li V, Feng F, Li S, Han Y. Computer simulation on the performance of a combined-type vertical axis wind turbine. In: Proceedings of the IEEE international conference on computer design and appliations (ICCDA): Qinhuangdao, Hebei, China; 25–27 June 2010.

[47] Yaakob OB, Tawi KB. Sunanto DTS. Computer simulation studies on the effect overlap ratio for Savonius type vertical axis marine current turbine. International Journal of Engineering Transactions A: Basics 2010;23(1):79–88.

[48] Afungchui D, Kamoun B, Helali A, Djemaa AB. The unsteady pressure field and the aerodynamic performances of a Savonius rotor based on the discrete vortex method. Renewable Energy 2010;35(1):307–13.

[49] Blackwell BF, Sheldahl RE, Feltz LV. Wind tunnel performance data for two- and three-bucket Savonius rotors. 1–105 Sandia laboratories report: SAND 76–0131.

[50] Can K, Feng Z, Xuejun M. Comparison study of a vertical-axis spiral rotor and a conventional Savonius rotor. In: Proceedings of the IEEE power and energy engineering conference (APPEEC): Chengdu, China; 28–31 March 2010.

[51] Launder BE, Spalding DB. The numerical computation of turbulent flows. Computer Methods in Applied Mechanics and Engineering 1974;3(2):269–89.

[52] Pope K, Rodrigues V, Doyle R, Tsopelas A, Gravelsins R, Naterer GF, et al. Effects of stator vanes on power coefficients of a zephyr vertical axis wind turbine. Renewable Energy 2010;35(5):1043–51.

[53] Debnath BK, Biswas A, Gupta R. CFD analysis of three-bucket Savonius rotor using Fluent package. In: Proceedings of national conference on recent advances in mechanical engineering: NIT Silchar, India; 20–21 December 2008.

[54] Debnath BK, Biswas A, Gupta RCFD. Analysis of combined three-bucket Savonius and three-bladed Darrieus rotor using Fluent package. In: Proceedings of international conference on advances in mechanical engineering: SVNIT, Surat, India; 16–17 December, 2008.

[55] Kamoji MA, Kedare SB, Prabhu SV. Performance tests on helical Savonius rotor. Renewable Energy 2009;34(3):521–9.

[56] Emmanuel B, Jun W. Numerical study of a six-bladed savonius wind turbine. Journal of Solar Engineering 2011;133:1–5.
[57] Roy S, Saha UK. Comparative analysis of turbulence models for flow simulation around a vertical axis wind turbine. In: Proceedings of the Indo-Danish international conference on wind energy: Materials, Engineering, and Policies (WEMEP 2012): Hyderabad, India; 22–23 November, 2012.
[58] Menter FR. Zonal two-equation k–ω turbulence models for aerodynamic flows. In: Proceedings of the 24th AIAA Fluid Dynamics Conference, Orlando, FL; 6–9 July 1993.
[59] Menter FR. Two-equation eddy-viscosity turbulence models for engineering applications. AIAA Journal 1994;32(8):1598–605.
[60] Plourde BD, Abraham JP, Mowry GS. Simulations of three-dimensional vertical axis turbines for communication applications. Wind Engineering 2012;36 (4):443–54.
[61] Spalart PR, Jou WH, Strelets M, Allmaras SR. Comments on the feasibility of LES for wings, and on a hybrid RANS/LES approach. In: Proceedings of the First AFOSR international conference on DNS/LES, Ruston, LA; 4–8 August 1997.
[62] Kalogirou SA. Artificial neural networks in renewable energy applications: a review. Renewable and Sustainable Energy Reviews 2001;5(4):373–401.
[63] Sargolzaei J. Prediction of the power ratio in the wind turbine Savonius rotor using artificial neural networks. International Journal of Energy and Environment 2007;2(1):51–6.
[64] Sargolzaei J, Kianifar A. Modeling and simulation of wind turbine Savonius rotors using artificial neural networks for estimation of the power ratio and torque. Simulation Modelling Practice and Theory 2009;17(7):1290–8.
[65] Sargolzaei J, Kianifar A. Neuro-fuzzy modelling tools for estimation of torque in Savonius rotor in wind turbine. Advances in Engineering Software 2010;41 (4):619–26.
[66] Jiang C, Yan Q. Study on the comparison between the horizontal axis and vertical axis wind turbine. ShangHai Electricity 2007;2:163–5.
[67] Kianifar A, Anbarsooz M. Blade curve influences on the performance of Savonius rotors: experimental and numerical. Proceedings of the Institution of Mechanical Engineers, Part A: Journal of Power and Energy 2011;225 (3):343–50.
[68] Alexander AJ, Holownia BP. Wind tunnel test on a Savonius rotor. Journal of Wind Engineering and Industrial Aerodynamics 1978;3(4):343–51.
[69] Gupta R, Biswas A, Sharma KK. Comparative study of three-bucket Savonius rotor with a combined three-bucket Savonius-three bladed Darrieus rotor. Renewable Energy 2008;33(9):1974–81.
[70] Huda MD, Selim MA, Sadrul Islam AKM, Islam MQ. The performance of an s-shaped Savonius rotor with a deflecting plate. RERIC International Energy Journal 1992;14(1):25–32.
[71] Saha UK, Thotla S, Maity D. Optimum design configuration of Savonius rotor through wind tunnel experiments. Journal of Wind Engineering and Industrial Aerodynamics 2008;96(8–9):1359–75.
[72] Shikha TS, Kothari DP. Wind energy conversion systems as a distributed source of generation. ASCE Journal of Energy Engineering 2003;129(3):69–80.